Fine-tuning molecular acoustic models: sensitivity of the predicted attenuation to the Lennard–Jones parameters

Andi G. Petculescu and Richard M. Lueptow[a)]
Department of Mechanical Engineering, Northwestern University, 2145 Sheridan Rd, Evanston, Illinois 60208 USA

(Received 7 July 2004; revised 30 September 2004; accepted 8 October 2004)

In a previous paper [Y. Dain and R. M. Lueptow, J. Acoust. Soc. Am. **109**, 1955 (2001)], a model of acoustic attenuation due to vibration-translation and vibration-vibration relaxation in multiple polyatomic gas mixtures was developed. In this paper, the model is improved by treating binary molecular collisions via fully pairwise vibrational transition probabilities. The sensitivity of the model to small variations in the Lennard–Jones parameters—collision diameter (σ) and potential depth (ϵ)—is investigated for nitrogen-water-methane mixtures. For a $N_2(98.97\%)$-$H_2O(338\,\text{ppm})$-$CH_4(1\%)$ test mixture, the transition probabilities and acoustic absorption curves are much more sensitive to σ than they are to ϵ. Additionally, when the 1% methane is replaced by nitrogen, the resulting mixture [$N_2(99.97\%)$-$H_2O(338\,\text{ppm})$] becomes considerably more sensitive to changes of σ_{water}. The current model minimizes the underprediction of the acoustic absorption peak magnitudes reported by S. G. Ejakov *et al.* [J. Acoust. Soc. Am. **113**, 1871 (2003)]. © *2005 Acoustical Society of America.* [DOI: 10.1121/1.1828547]

PACS numbers: 43.35.Ae, 43.35.Fj, 43.20.Hq [RR] Pages: 175–184

I. INTRODUCTION

In a gaseous medium, the molecules exchange energy via collisions. Excitation—relaxation processes transfer energy between internal (e.g., vibrational, rotational) and external (translational) degrees of freedom, and/or among internal degrees of freedom. Upon the passage of a sound wave, excited molecules do not exchange vibrational and/or rotational energy infinitely fast with the translational degrees of freedom associated with the temperature fluctuations. As a result, the total specific heat of the relaxing gas becomes complex valued and frequency dependent. Sound propagation is characterized by a frequency-dependent and complex-valued effective wave number, the real and imaginary parts of which yield the speed of sound and attenuation, respectively. In typical molecular acoustics experiments, the absorption and sound speed are measured over a frequency range within which the expected relaxation processes occur. From these curves, the relaxation times can be extracted and gas-kinetic properties such as collision rates and transition probabilities can be calculated. The present work, on the other hand, is motivated by the need for fast acoustic monitors for gaseous processes based on algorithms that track changes in the relaxation characteristics of gas mixtures.[1,2] As a result, it is critical to be able to predict the acoustic propagation characteristics for a wide range of molecular species.

The complex process in which the molecules change state upon collision is described analytically by quantum-mechanical inelastic scattering theory. The interaction is governed by an intermolecular potential typically characterized by a long-range attractive part and a short-range repulsive ''core.'' At present, the complex nature of the forces acting between molecules is not completely understood. The attraction forces (van der Waals or London dispersion forces) are thought to arise from the electric fields induced in each molecule by their rapidly fluctuating electric dipoles,[3] while other theories advocate the attraction forces between nuclei and their distorted electron clouds.[4] At very small separations, it is conjectured that the electronic clouds of the ''collision'' pair overlap, thus leading to strong, short-ranged repulsion.[5] The Lennard–Jones (or 12-6) intermolecular potential function has been used quite successful in modeling many nonpolar or weakly polar gases. Depending on the structure of the gas molecules and the ambient conditions, the Lennard–Jones potential can be supplemented by other interaction terms describing multipole electrostatic fields, induction fields between permanent dipoles and/or quadrupoles, chemical forces, etc.[5] Depending on the complexity of the interactions involved, other intermolecular potentials may be used.[5]

The relaxation times depend on the probabilities of transition between different quantum states after a collision. The transition probabilities, in turn, are contingent upon the form of the intermolecular potential. Ultimately, it is the interaction potential that will dictate the response of the gas to acoustic forcing. In a pioneering semiclassical approach to connect molecular transfer rates and the acoustic dispersion equation, Landau and Teller[6] used an exponential repulsive potential, arguing that the long-range attractive forces are unimportant for transitions. Based on the equidistant harmonic oscillator levels, they assumed that all relaxation processes occur effectively with a single relaxation time. Simultaneously, they advanced the concept of a *transition-favorable incident velocity*. For each temperature, out of the Maxwell distribution of incident velocities, a certain value can be picked out that maximizes the probability of quantum jumps. The salient feature of the Landau–Teller model is that only the molecules entering the interaction region with ve-

a)Corresponding author; electronic mail: r-lueptow@northwestern.edu

locities lying in the vicinity of the transition-favorable value are likely to induce transitions. Jackson and Mott[7] had developed the distorted-wave method for the quantum-mechanical treatment of inelastic scattering from an exponential potential. Through its purely repulsive (positive-valued) potential, the Landau–Teller model was able to predict the behavior of certain gases with varying degrees of success.

Shields[8] showed that the Landau–Teller approach using an exponential repulsive potential adequately predicts the temperature dependence of transition probabilities in CO_2. However, by not accounting for the attractive forces between molecules, the model is not widely applicable. On the other hand, using the Lennard–Jones function instead of an exponential can lead to mathematically intractable integrals since the transition probabilities involve calculation of the matrix elements of the scattering potential. That is why a substitute for the Lennard–Jones potential was sought in the form of a shifted exponential potential function that has both positive (repulsion) and negative (attraction) values and whose slope (force) and/or magnitude are adjusted to match those of the Lennard–Jones potential at specific points.[9] In this picture, the incident molecule is accelerated under the influence of a quasiuniform attractive potential until it enters the range of the strong repulsive ''core,'' shedding its kinetic energy at the classical turning point (or closest approach point).

Schwartz, Slawsky, and Herzfeld (SSH)[10] used the distorted-wave method to calculate vibration-translation and vibration-vibration transition probabilities by replacing the one-dimensional Lennard–Jones potential by a *shifted exponential function* tangent to the former at the classical turning point for the transition-favorable incident velocity. The SSH model addresses the problem of multiple relaxation times through the concept of complex interactions, in which each collision partner makes a single-quantum jump to a different vibrational state. Schwartz and Herzfeld[11] later extended the problem to three dimensions for diatomic molecules.

The choice of the classical turning point is not arbitrary; in general terms, it represents the molecular separation where the actual ''collision'' occurs. Herzfeld and Litovitz[9] pointed out that fitting the potential function at the classical turning point and at the zero-potential point, or collision diameter (for the hard-sphere approximation, this is the effective diameter of the colliding ''spheres''), results in better agreement with data than fitting the potential energy function and its slope (force) at the classical turning point. Tanczos[12] extended the SSH model further to include two-quantum exchanges for polar polyatomic molecules, specifically chloromethanes. He applied the SSH fitting method to the Krieger potential[13] for polar molecules. However, inconsistencies between the theory and measurements resulted due to the fact that the Krieger function does not accurately model collisions between polar molecules, as pointed out by Monchick and Mason.[14] Shields[15] described qualitatively the path of the relaxation processes—series (relaxation occurs in steps, via intermediary energy levels) or parallel (each excited level relaxes separately)—by resorting to electrical circuit analogs. In addition, he discussed the sensitivity of the absorption/dispersion curves to the relaxation path. Bauer *et al.*[16] developed a generalized model for acoustic dispersion and attenuation in binary polyatomic gas mixtures that allows for multi-quanta vibrational relaxation.

While the volume of theoretical and experimental work that has been done in the field of nonclassical attenuation and dispersion of sound in gases is impressive, a common thread that runs through many models is that they require one or more free parameters in order to match the experimental data. In the case of multicomponent mixtures, the large number of factors that affect the transition probabilities acts to hinder the development of universal predictive models. That is why systematic studies aimed at identifying the aforementioned factors are warranted. Moreover, the operation of a potential real-time acoustic gas sensor[1,2] would have to be sensitive to changes in the absorption and phase velocity as the composition varies (e.g., from leaks or foreign gases). Recently, Dain and Lueptow (DL)[17,18] extended the SSH theory to model vibrational relaxation in ternary mixtures of polyatomic gases at room temperature. While their results compared favorably with experimental data, there is clearly room for improvement in the model.

The goal of this paper is to investigate the sensitivity of the nonempirical DL model, based on the SSH theory, to small variations in the Lennard–Jones parameters. Since the SSH theory is based on vibration-translation and vibration-vibration relaxation and our focus is on processes at room temperature, we do not consider vibration-rotation and rotation-translation relaxation, which typically are important at high temperatures.[19–22] In addition, a minor oversight in the DL model is corrected and the DL model is refined by using full pairwise parametrization of two-molecule collisions. The gases chosen for the study are nitrogen, methane, and water vapor because they were studied in the original DL model and because they have practical implications for an acoustic gas sensor. Of the three species, perhaps the most ''troublesome'' is water vapor. A large number of publications have been devoted to understanding the forces arising between water molecules. Given the breadth of the work on water properties, which has yielded a wide range of results for the intermolecular forces,[23] it is only natural to determine the sensitivity of a particular relaxation model to the choice of the water force constants. Nitrogen is also of interest, for two reasons: it is the heaviest of the three species, and it has the lowest vibrational amplitude. In this paper, the Lennard–Jones (LJ) force constants are varied over ranges that agree with the bounds set by published data. The central part of the analysis consists of determining (i) the amount of change induced in and (ii) the functional dependence of the transition probabilities and relaxation frequencies as the force constants of water and nitrogen are changed incrementally. Then the sensitivity of the predicted attenuation to the force constants is evaluated.

II. SHIFTED-EXPONENTIAL APPROXIMATION OF THE LENNARD-JONES POTENTIAL

The core of a relaxational theory is the calculation of transition probabilities. These are based on the quantum-mechanical treatment of the inelastic scattering of molecules of species *a*, initially in vibrational state i_a from a ''target'' of species *b*, initially in state i_b. After the ''collision,'' mol-

ecules a are in the final state f_a and molecules b are in the final state f_b. The interaction potential $V_{ab}(\mathrm{r})$ is approximated by the Lennard–Jones (LJ) function

$$V_{LJ}(r)=4\epsilon_{ab}[(\sigma_{ab}/r)^{12}-(\sigma_{ab}/r)^{6}], \tag{1}$$

where r is the molecular separation, and ϵ_{ab} and σ_{ab} are the pairwise potential depth and the zero-potential point (or collision diameter), respectively. The latter are defined in terms of the ''individual'' parameters (describing collisions between like molecules)[24]

$$\epsilon_{ab}\equiv(\epsilon_{aa}\epsilon_{bb})^{1/2} \quad \text{and} \quad \sigma_{ab}\equiv(\sigma_{aa}+\sigma_{bb})/2. \tag{2}$$

Schwartz and Herzfeld[11] fit the magnitude and slope of a shifted exponential function to the Lennard–Jones potential at the point of closest approach or classical turning point r_c, for the transition-favorable incident velocity v_0^*. The shifted-exponential fit is given by

$$V_{\exp}(r)=(\epsilon_{ab}+E^*)e^{\alpha^*_{ab}(r_c-r)}-\epsilon_{ab}. \tag{3}$$

$E^*\equiv\mu v_0^{*2}/2$, where $\mu\equiv m_a m_b/(m_a+m_b)$ is the reduced mass of the collision pair, m_a and m_b are the masses of the interacting molecules, and α^*_{ab} is the decay parameter of the exponential function (we will refer to α^*_{ab} subsequently as the repulsion parameter). The key fitting point for the Lennard–Jones and exponential functions is the classical turning point r_c, where all the kinetic energy of the incident molecules E^* is converted into potential energy. The second fitting point is the hard-sphere collision diameter σ_{ab} [for which $V_{\mathrm{LJ}}(\sigma_{ab})=V_{\exp}(\sigma_{ab})=0$]. The two potential functions are matched iteratively. Starting with arbitrary initial values for the ''input'' variables r_c and α^*_{ab}, both variables are varied until $V_{\exp}(\sigma_{ab})=V_{LJ}(\sigma_{ab})=0$ and $V_{\exp}(r_c)=V_{\mathrm{LJ}}(r_c)=E^*$. Matching the two potential functions [Eqs. (1) and (3)] as described above establishes an intimate interconnectedness between the Lennard–Jones parameters (ϵ_{ab} and σ_{ab}), the shifted exponential parameters (r_c and α^*_{ab}), and, as will become apparent later, the transition probabilities. It is this very interconnectedness that the present paper aims to bring to light.

As an example, Fig. 1 shows the shifted exponential function [Eq. (3)] matched to the Lennard–Jones potential [Eq. (1)] for N_2-H_2O collisions using $\sigma_{12}=4.086$ Å and $r_c=3.604$ Å, where subscripts 1 and 2 refer, respectively, to N_2 and H_2O (see Table II). For clarity, the intermolecular potential and separation are normalized to the LJ depth $\epsilon_{12}=2.415\times10^{-21}$ J and the collision diameter σ_{12}, respectively. For the N_2-H_2O pair, $v_0^*=1593.2$ m/s, $E^*=2.310\times10^{-20}$ J, and $\alpha^*_{12}=4.887\ \text{Å}^{-1}$. It is quite clear that the shifted exponential function is a good approximation of the repulsive part of the Lennard–Jones potential ($r<\sigma_{12}$). The molecules lose their kinetic energy until they reach the classical turning point r_c which, for this particular case, is $0.88\sigma_{12}$. For the attractive portion of the potential energy ($r>\sigma_{12}$), the exponential function matches the LJ potential reasonably well in the vicinity of the Lennard–Jones well depth. Under the action of the shifted exponential potential, molecules coming in from infinity experience almost uniform attraction until the separation distance equals the zero-potential value σ_{12}. The discrepancy between the Lennard–Jones potential and the shifted exponential function at large r is inconsequential, since the collisions are assumed to be effective only at small separations, in the vicinity of the classical turning point.[6,10]

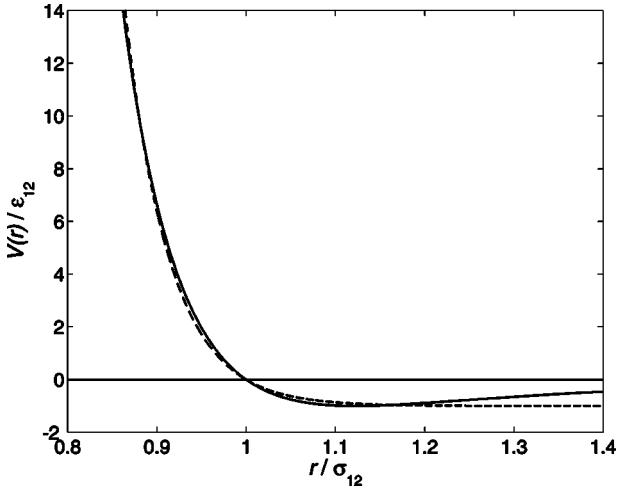

FIG. 1. The shifted exponential (dashed) and Lennard–Jones (solid) functions matched at $r=\sigma_{12}$ and $r=r_c\approx0.88\sigma_{12}$, for N_2-H_2O collisions at $T=300$ K. The repulsion parameter is $\alpha^*_{12}=4.887\ \text{Å}^{-1}$.

The parameters for the exponential function are incorporated into the expression for the transition probability, which is, after being corrected by Tanczos,[12]

$$P^{i_a\to f_a}_{i_b\to f_b}(a,b)=P_0(a)P_0(b)\frac{1.364}{1+C/T}\left(\frac{r_c}{\sigma_{ab}}\right)^2\overline{V}^2_{i_a,f_a}\overline{V}^2_{i_b,f_b}\times8\sqrt{\frac{\pi}{3}}\left(\frac{2\pi\mu\Delta E}{\alpha^{*2}_{ab}\hbar^2}\right)^2\zeta_{ab}^{1/2}\times\exp\left[-3\zeta_{ab}+\frac{\Delta E}{2k_BT}+\frac{\epsilon_{ab}}{k_BT}\right], \tag{4a}$$

where

$$\zeta_{ab}\equiv\frac{\mu v_0^{*2}}{2k_BT}=\left(\frac{\Delta E^2\mu\pi^2}{2\alpha^{*2}_{ab}\hbar^2k_BT}\right)^{1/3}. \tag{4b}$$

$\Delta E=\hbar\omega_a(i_a-f_a)+\hbar\omega_b(i_b-f_b)$ is the energy exchanged with translational degrees of freedom during a collision process, ω_a and ω_b are the vibrational angular frequencies, $P_0(a)$ and $P_0(b)$ are nonsphericity (or steric) factors, C is the Sutherland constant, $\hbar=1.0546\times10^{-34}$ Js is the reduced Planck's constant, $k_B=1.3807\times10^{-23}$ J/K is the Boltzmann constant, and T is the temperature in degrees kelvin. The vibrational factors $\overline{V}^2_{i,f}$ factors represent the squares of the transition matrix elements between the i and f harmonic oscillator states for each molecular species. For zero- and one-quantum jumps, the vibrational factors for species a are[10]

$$\overline{V}^2_{i_a,f_a}=\begin{cases}1, & \text{for } f_a=i_a\\ (i_a+1/2\pm1/2)(\alpha^*_{aa})^2\overline{A}^2\hbar/2\omega_a, & \text{for } f_a=i_a\pm1\end{cases}, \tag{5}$$

TABLE I. Normal modes of vibration, mode degeneracies, and vibrational amplitude coefficients for N_2, H_2O, and CH_4 from Ref. 25. The modes in bold type are those assumed to be active around room temperature.

Species	Normal modes (cm^{-1})		g	$\overline{V^2}$ (amu^{-1})
N_2	ν	**2331**	**1**	**0.0354**
H_2O	ν_1	3657	1	0.9539
	ν_2	**1596**	**1**	**0.9527**
	ν_3	3756	1	0.9241
CH_4	ν_1	2915	1	0.9921
	ν_2	**1534**	2	**0.9921**
	ν_3	3019	1	0.9923
	ν_4	**1306**	3	**0.8368**

where $\overline{A^2}$ is the vibrational amplitude coefficient representing the averaged displacement of surface atoms for unit change of the normal coordinate for a given vibration.[25] Inherent in the probabilities as described by Eq. (4a) is the existence of two ways in which the exchange of translational and vibrational energy occurs. First, there are processes whereby only one collision partner changes vibrational state. For example, the probability of molecule a losing one quantum ($i_a=1\rightarrow f_a=0$) while the vibrational state of molecule b is unaltered ($i_b=0\rightarrow f_b=0$) would be described by $P_{00}^{10}(a,b)$, or simply $P^{10}(a,b)$, where the arrows in the superscript and subscript have been omitted. This process, where a single quantum is exchanged with translation, is called a ''vibration-translation,'' or V-T, interaction. Second, complex collisions may exist in which *both* partners gain/lose one quantum each, the difference $\hbar\omega_a-\hbar\omega_b$ being changed into kinetic energy.[9] Such a process, where a total of two quanta are exchanged with translation and which is described by the probability $P_{01}^{10}(a,b)$, is called a ''vibration-vibration,'' or V-V, interaction.

Equations (3), (4a), and (4b) show explicitly the sensitivity of a relaxational model to the values of the parameters ϵ_{ab}, σ_{ab}, α_{ab}^*, and r_c. Because of the matching procedure, the LJ collision diameter (σ_{ab}) and potential well depth (ϵ_{ab}) are interconnected with the repulsion parameter α_{ab}^* and the classical turning point r_c of the shifted exponential function. As a result, a change in σ_{ab} or ϵ_{ab} leads immediately to changes in α_{ab}^* and r_c, which in turn affect the transition probabilities. This dependence of the transition probabilities on the force constants and their impact on acoustic propagation in gas mixtures are the focus of this study.

As in Ref. 17, a mixture of water vapor, methane, and nitrogen is considered. Table I provides the vibrational modes, degeneracies g, and vibrational coefficients of nitrogen, water, and methane. At temperatures around 300 K, it is assumed that only the lowest modes are significant. The contribution of higher modes to molecular energy transfer at these temperatures is small. Consequently, it is assumed that energy exchange will occur with a high probability only between the following vibrational modes: $\nu=2331\ cm^{-1}$ of N_2, $\nu_2=1596\ cm^{-1}$ of H_2O, and $\nu_2=1534\ cm^{-1}$ and $\nu_4=1306\ cm^{-1}$ of CH_4. The second vibrational mode $\nu_2=1534\ cm^{-1}$ of CH_4 is included in the relaxation process due to its near resonance with the mode $\nu_2=1596\ cm^{-1}$ of H_2O. In the analysis, the following indices are used: 1 for N_2, 2 for $H_2O(\nu_2)$, 3 for $CH_4(\nu_4)$, and 4 for $CH_4(\nu_2)$, as in Ref. 17.

TABLE II. Reference parameters for the Lennard–Jones and exponential potentials (the values for σ_{aa} and ϵ_{aa} ($a=1...4$) are similar to those used in Refs. 17 and 18, based on Ref. 5). The quantities that will change in the analysis are shown in boldface.

Pair (ab)	σ_{ab} (Å)	ϵ_{ab}/k_B (K)	α_{ab}^* ($Å^{-1}$)	r_c (Å)
11	***3.704***	***80.01***	**5.093**	**2.941**
22	***4.468***	***382.43***	**4.530**	**4.002**
33	*4.075*	*143.91*	4.796	3.490
44	*4.075*	*143.91*	4.775	3.465
21; **12**	**4.086**	**174.92**	**4.887**	**3.604**
23; **32**	**4.271**	**234.60**	**4.924**	**3.965**
24; **42**	**4.271**	**234.60**	**5.207**	**4.118**
31; **13**	**3.890**	**107.3**	**4.989**	**3.292**
34; 43	4.075	143.91	5.081	3.733
41; **14**	**3.890**	**107.31**	**5.023**	**3.328**

In the present sensitivity analysis, the Lennard–Jones potential parameters for nitrogen ($\sigma_{11},\epsilon_{11}$) and water ($\sigma_{22},\epsilon_{22}$) are varied from the original values used in Ref. 17, which are based on viscosity.[5] As a result, the parameters σ_{ab} and ϵ_{ab} for all the interactions except those between the two CH_4 modes will change; for every interaction pair, the repulsion parameter α_{ab}^* is determined by matching the associated exponential and LJ potentials as described following Eq. (3). Table II provides the reference values of the Lennard–Jones force constants and the corresponding exponential fit parameters for the four vibrational modes. The original model described in Refs. 17 and 18 used only the italicized quantities in Table II. For the model described here, all of the values in Table II are used in an effort to improve accuracy. Boldface indicates the values that will change in the analysis. The values for α_{aa}^* used in the original DL model were slightly different than those shown in Table II (within 2% for nitrogen and methane, and 6% for water). Also, in the original DL model, the classical turning point was not used explicitly. Instead, the ratio $(r_c/\sigma_{aa})^2$ was approximated by imposing $V_{LJ}(r_c)\approx k_BT$. Only the values in the first two lines of Table II will be varied systematically; the other boldface values will change as a result of varying the ''11'' and ''22'' values.

In the first step of the analysis, the LJ force constants of water are kept constant ($\sigma_{22}=4.468$ Å, $\epsilon_{22}/k_B=382.43$ K) while the values of σ_{11} and ϵ_{11}/k_B of nitrogen are allowed to vary, in turn, from 3.334 to 3.704 Å, and from 80.01 to 96.01 K, respectively. In the second step, the force constants for N_2 are held constant ($\sigma_{11}=3.704$ Å, $\epsilon_{11}/k_B=80.01$ K) and those of H_2O are allowed to change: σ_{22} from 3.217 to 4.468 Å, and, separately, ϵ_{22}/k_B from 302.12 to 474.21 K. The directions of variation of the water and nitrogen force constants are such that, starting from initial reference values used in Table II, they stay within the ranges found in the literature.[5,14,23] Thus σ_{11} varies between 3.334 and 3.704 Å, ϵ_{11}/k_B between 80.01 and 96.01 K, σ_{22} between 3.217 and 4.468 Å, and ϵ_{22}/k_B between 302.12 and 474.21 K for water. Values of $\sigma_{22}<3$ Å and $\epsilon_{22}/k_B>700$ K appear in the literature but they often involve nonphysical assumptions such as

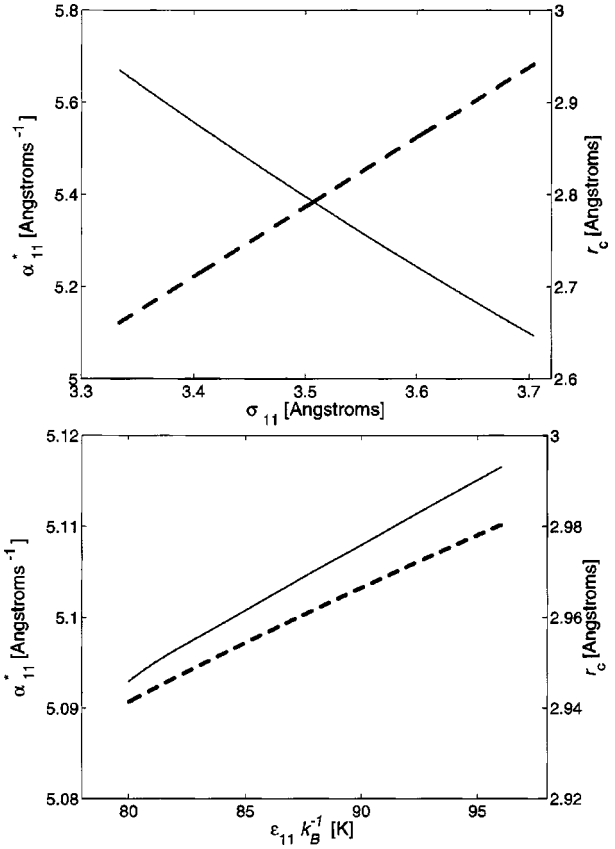

FIG. 2. Variation of the nitrogen repulsion parameter α_{11}^{*} (solid) and closest approach point r_c (dashed) with the nitrogen collision diameter, σ_{11} (top), and with the nitrogen LJ potential depth, ϵ_{11} (bottom).

embedded point dipoles[14] and/or single-point interactions,[23] so they are not considered here.

The transition probabilities do not have an explicit functional dependence on the LJ potential parameters, σ and ϵ. Changes in σ and ϵ alter the shifted-exponential repulsion parameter α^* and the classical turning point r_c, which also enter the expression for the transition probabilities. Therefore, an analysis of the sensitivity to values of σ and ϵ should start with showing how these parameters affect α^* and r_c. Figure 2 shows the dependence of the N_2-N_2 repulsion parameter (α_{11}^{*}) and turning point (r_c) on σ_{11} and ϵ_{11}. It is clear that α_{11}^{*} and r_c vary monotonically with σ_{11} and ϵ_{11} over the parameter range found in the literature.

Of course, the interspecies transition probabilities involving nitrogen will also be affected by the variation in these parameters, according to Eqs. 4(a), and 4(b). It is these transition probabilities that affect the acoustic attenuation and dispersion in gas mixtures, which are the focus of this study. Figure 3 shows selected transition probabilities as a function of the corresponding pairwise LJ parameters [for the sake of brevity, only N_2-N_2 ("1,1") and N_2-H_2O ("1,2") cases are shown; transition probabilities between nitrogen and the two modes of methane exhibit a behavior similar to that of Figs. 3(b) and 3(d)]. The dependence of the transition probabilities on pairwise collision diameter σ_{11} is notably nonlinear for the V-T collisions among nitrogen molecules [$P^{10}(1,1)$]. The dependence on σ_{12} is only slightly nonlinear for the V-V nitrogen-water interaction $P_{01}^{10}(1,2)$. The results

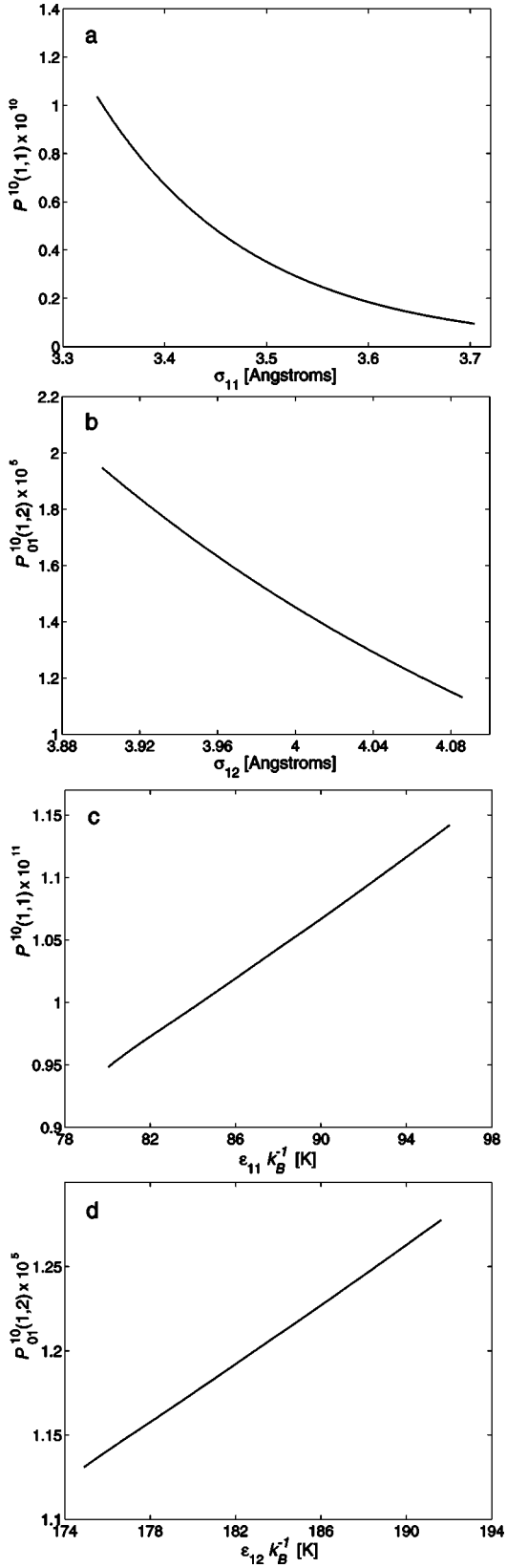

FIG. 3. The effects of varying the N_2 force constants ϵ_{11} and σ_{11} on transition probabilities for N_2-N_2 ("1,1") and N_2-H_2O ("1,2") collisions. (a) dependence V-T probability dependence on σ_{11}, for $\sigma_{22}=4.468$ Å, (b) V-V probability dependence on σ_{12}, for $\sigma_{22}=4.468$ Å, (c) V-T probability dependence on ϵ_{11}/k_B, for $\epsilon_{22}/k_B=382.43$ K, and (d) V-V probability dependence on ϵ_{12}/k_B, for $\epsilon_{22}/k_B=382.43$ K. Note the considerably larger sensitivity to the values of the collision diameters.

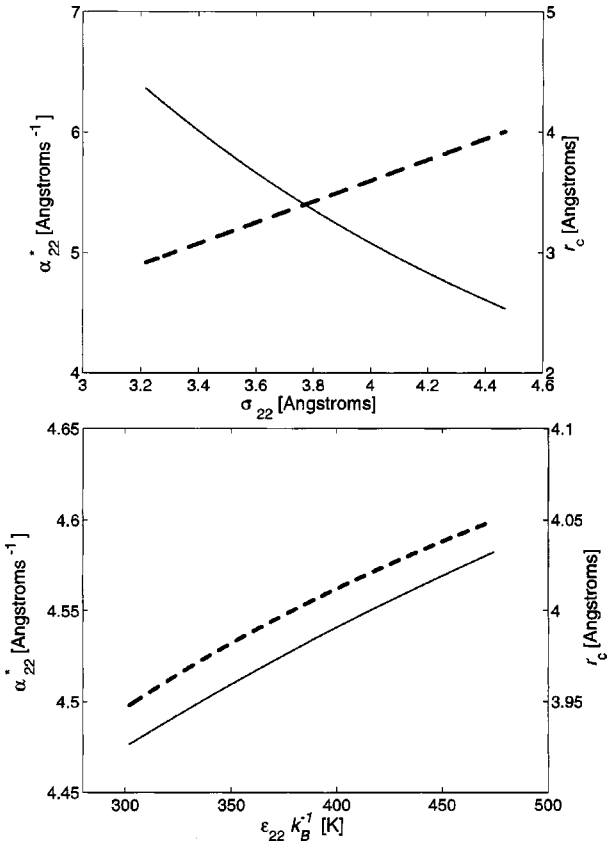

FIG. 4. Variation of the water repulsion parameter α_{22}^{*} (solid) and closest approach point r_c (dashed) with the water collision diameter, σ_{22} (top), and with the water LJ potential depth, ϵ_{22} (bottom).

for $P_{01}^{10}(2,1)$, which are not shown, are similar to those for $P_{01}^{10}(1,2)$. The transition probabilities increase nearly linearly over the range of the potential depths (ϵ_{11} and ϵ_{12}). The more important observation, however, is that the transition probabilities are quite sensitive to variations in the collision diameters, varying by a factor of almost 11 for $P^{10}(1,1)$ and a factor of almost 2 for $P_{01}^{10}(1,2)$ and $P_{01}^{10}(2,1)$. The transition probabilities are much less sensitive to variations in the potential depths, varying by less than 20%.

The dependence of the repulsion parameters and turning points, and of selected transition probabilities on the water force constants are shown in Figs. 4 and 5, respectively. Figure 4 shows the dependence of the H_2O-H_2O (“22”) repulsion parameter (α_{22}^{*}) and turning point (r_c) on σ_{22} and ϵ_{22}. Again, α_{22}^{*} and r_c vary monotonically with σ_{22} and ϵ_{22} in the range that is considered. The transition probabilities have a nonlinear dependence on the collision diameters [notably so for $P^{10}(2,2)$ for V-T transitions among water molecules]. In this case, the dependence of the V-T probability on the potential depth ϵ_{22}/k_B is also somewhat nonlinear, although the dependence of the V-V probability is nearly linear. Again, it is evident from Fig. 5 that the transition probabilities are quite sensitive to changes in the collision diameters [a factor of almost 127 for $P^{10}(2,2)$ and a factor of nearly 6 for $P_{01}^{10}(1,2)$]. However, the V-T transition probability is also quite sensitive to the potential depth of water ϵ_{22}/k_B, unlike the dependence on the potential depth of nitrogen ϵ_{11}/k_B.

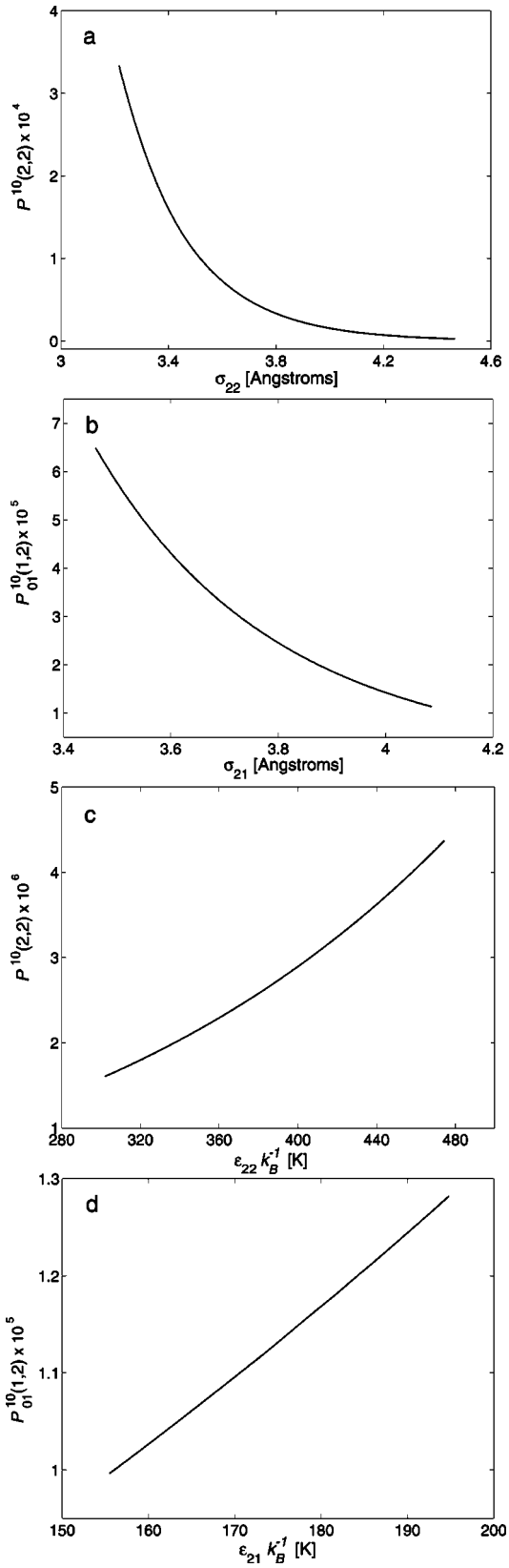

FIG. 5. The effects of varying the H_2O force constants ϵ_{22} and σ_{22} on transition probabilities for H_2O-H_2O (“2,2”) and N_2–H_2O (“1,2”) collisions. (a) V-T probability dependence on σ_{22}, for $\sigma_{11}=3.704$ Å, (b) V-V probability dependence on $\sigma_{21}(=\sigma_{12})$, for $\sigma_{11}=3.704$ Å, (c) V-T probability dependence on ϵ_{22}/k_B, for $\epsilon_{11}=80.01$ K and (d) V-V probability vs $\epsilon_{21}/k_B(=\epsilon_{12}/k_B)$, for $\epsilon_{11}=80.01$ K. Note the considerably larger sensitivity to values of the collision diameters.

III. SENSITIVITY OF ACOUSTIC ATTENUATION TO LENNARD–JONES PARAMETERS

The DL model[17] is centered on the set of relaxation equations

$$\frac{d\Delta T^{\mathrm{vib}}}{dt} = -\mathbf{A}\Delta T^{\mathrm{vib}} + \mathbf{q}\Delta T, \tag{6}$$

where ΔT^{vib} and ΔT are the fluctuations of the vibrational and translational temperatures, respectively, with respect to the equilibrium temperature T_0. $\mathbf{q}$ is a vector and $\mathbf{A}$ is the 4×4 relaxation matrix incorporating the inverses of the relaxation times (effective relaxation frequencies). Their components are given by the following relations:[17]

$$q_a = \frac{1}{\tau_a^{VT}} + \sum_{\substack{b=1\\ b\neq a}}^{4} \frac{1}{\tau_{a,b}^{VV}} \frac{1-\exp(-\hbar\omega_a/k_BT_0)}{1-\exp(-\hbar\omega_b/k_BT_0)}\left[1-\frac{\omega_b}{\omega_a}\right], \tag{7}$$

$$A_{aa} = \frac{1}{\tau_a^{VT}} + \sum_{\substack{b=1\\ b\neq a}}^{4} \frac{1}{\tau_{a,b}^{VV}} \frac{1-\exp(-\hbar\omega_a/k_BT_0)}{1-\exp(-\hbar\omega_b/k_BT_0)},$$

$$a = 1,...,4,$$

$$A_{ab} = -\frac{1}{\tau_{a,b}^{VV}} \frac{1-\exp(-\hbar\omega_a/k_BT_0)}{1-\exp(-\hbar\omega_b/k_BT_0)} \frac{\omega_b}{\omega_a}, \tag{8}$$

$$a,b = 1,...,4, \quad a\neq b.$$

The translational (V-T) relaxation times that appear in Eq. (5) are

$$\frac{1}{\tau_a^{VT}} = \sum_{b=1}^{3} \frac{\alpha_b}{\tau_{a,b}^{VT}}, \quad a = 1,...,3,$$

$$\frac{1}{\tau_4^{VT}} = \sum_{b=1}^{2} \frac{\alpha_b}{\tau_{4,b}^{VT}} + \frac{\alpha_3}{\tau_{4,4}^{VT}} \tag{9}$$

where α_i are the molar fractions of the three species ($\alpha_4 = \alpha_3$, for the two methane modes considered). The paired V-T and V-V inverse relaxation times for excitation processes with one and two vibrational modes involved are, respectively,[17]

$$(\tau_{a,b}^{VT})^{-1} = Z(a,b)P^{10}(a,b)[1-\exp(-\hbar\omega_a/k_BT_0)]$$

$$(\tau_{a,b}^{VV})^{-1} = \alpha_b g_b Z(a,b)P_{01}^{10}(a,b), \quad a,b = 1,...,4, \tag{10}$$

$$a\neq b, \quad \alpha_3 = \alpha_4.$$

Here $Z(a,b)$ are the rates of collision of molecules of species a with molecules of species b. The collision rate per molecule is based on the kinetic theory for a gas of rigid spheres[25]

$$Z(a,b) = 2N_a\sigma_{ab}^2\sqrt{2\pi k_BT_0\frac{m_a+m_b}{m_am_b}}, \tag{11}$$

where N_a is the number density of the "a" molecules, and m_a, m_b are the molecular masses of the two species. The calculation of the effective acoustic wave number is described in detail in Ref. 17. It is set up from linear acoustic equations for ideal gases. Substitution of a harmonic plane-wave solution of the wave equation into Eq. (6) results in the following algebraic set of equations:[17]

$$(i\omega\mathbf{I}+\mathbf{A})\Delta T^{\mathrm{vib}} = \mathbf{q}\Delta T, \tag{12}$$

where $\mathbf{I}$ is the identity matrix. Equation (12) connects the temperature fluctuations of the internal (vibrational) and external (translational) degrees of freedom. The complex-valued, frequency dependent effective wave number is given by the following expression:

$$\tilde{k}^2 = k_0^2\frac{C_V^0+\Sigma_{i=1}^4\alpha_iC_i^{\mathrm{vib}}(\Gamma_i-1)}{C_P^0+\Sigma_{i=1}^4\alpha_iC_i^{\mathrm{vib}}(\Gamma_i-1)}, \tag{13}$$

where k_0, C_V^0, and C_P^0 are the static ($\omega\to0$) values of the wave number and the translational isochoric and isobaric specific heats of the mixture, respectively, C_i^{vib} is the vibrational specific heat of species i, and $\Gamma_i \equiv \Delta T_i^{\mathrm{vib}}/\Delta T_i$ is the temperature fluctuation ratio. The imaginary and real parts of the effective wave number $\tilde{k}$ determine the attenuation and phase velocity of the acoustic wave. The original model developed in Ref. 17 inadvertently used $C_V^0+\Sigma_{i=1}^4\alpha_iC_i^{\mathrm{vib}}\Gamma_i$ and $C_P^0+\Sigma_{i=1}^4\alpha_iC_i^{\mathrm{vib}}\Gamma_i$ instead of the corresponding expressions in the numerator and the denominator, respectively, of the right-hand side of Eq. (13). The correction moderately increases the magnitude of the theoretical attenuation peaks presented in Ref. 2. For example, for pure methane, the correction raises the height of the normalized attenuation peak by about 15%, to within 2% of the experimental data. Also for methane, using the pairwise model described in Sec. I reduces the disagreement between the predicted and measured attenuation peaks from 19% to 4%.

The model described by Eqs. (6)–(13) is applied to calculate the effective wave number, the imaginary and real parts of which yield the frequency-dependent acoustic absorption $\alpha(\omega)$ and speed of sound $c(\omega)$, in a mixture of $N_2(98.97\%)$-$H_2O(338\,\mathrm{ppm})$-$CH_4(1\%)$. This particular mixture was considered because experimental data is available for the acoustic attenuation over a range of frequencies,[27] it includes the effects of water vapor, and it was previously considered in Ref. 17. The sensitivity of the attenuation to changes in the water and nitrogen force constants is shown in Fig. 6. The LJ force constants are varied from their reference values (Table II), which happen to be near one end of the range of values in the literature, to values at the other end of the range. Specifically, σ_{11} and σ_{22} are varied from 3.704 to 3.334 Å (10%) and from 4.468 to 3.217 Å (28%), respectively, while ϵ_{11}/k_B and ϵ_{22}/k_B are varied from 80.01 Å to 96.01 K (20%) and from 382.43 K to 474.21 K (24%), respectively. The frequency/pressure ratios at which the absorption peaks occur in Fig. 6 are indicative of the relaxation processes occurring in the mixture; their relative magnitudes depend on the concentrations of the component molecular species. As a result, the magnitudes of the peaks are unaltered as the force constants are varied, but the relaxation frequencies do depend on the choice of the force constants, σ and ϵ. It is apparent that the attenuation of the mixture is considerably more sensitive to changes in σ_{11}, the collision diameter of nitrogen, than to σ_{22}, ϵ_{11} or ϵ_{22}. The

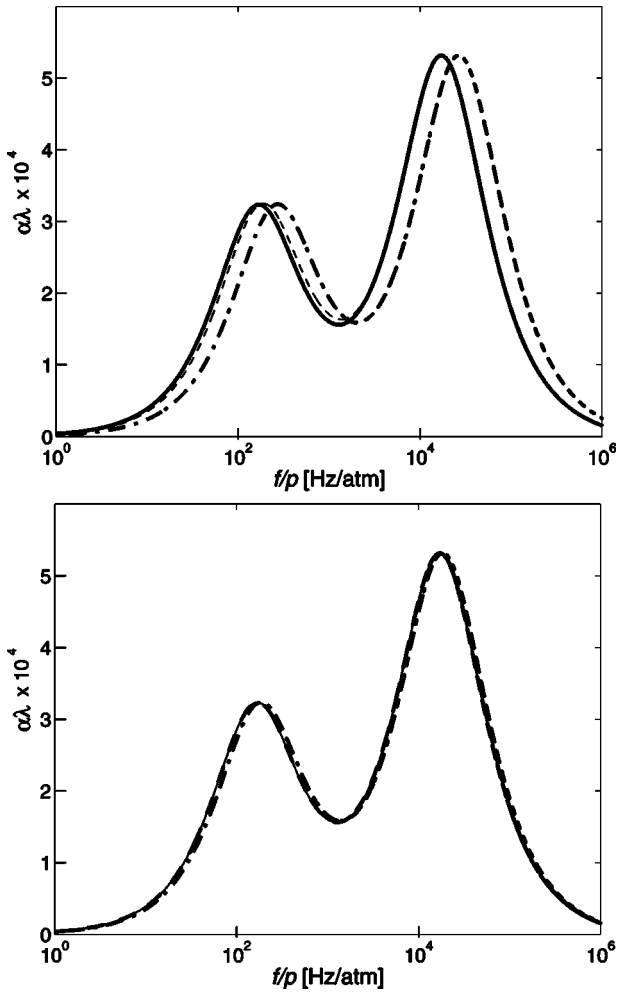

FIG. 6. Effects of the variation of the collision diameter and potential depth for the N_2(98.97%)-H_2O(338 ppm)-CH_4(1%) mixture on the attenuation nondimensionalized by the acoustic wavelength. Top: σ_{11} and σ_{22} are varied by 10% and 28%, respectively, from their reference values (Table II). Bottom: ϵ_{11}/k_B and ϵ_{22}/k_B are varied by 20% and 24%, respectively, from their reference values (Table II). Solid: using reference values ($\sigma_{11}=3.704$ Å, $\sigma_{22}=4.468$ Å, $\epsilon_{11}/k_B=80.01$ K, $\epsilon_{22}/k_B=382.43$ K). Dashed: effect of changing H_2O parameters, so that $\sigma_{22}=3.217$ Å and $\epsilon_{22}/k_B=474.21$ K, with σ_{11} and ϵ_{11}/k_B at their reference values. Note that the effect of changing ϵ_{11} is so small that the dashed is hidden by the solid curve in the lower figure. Dot-dashed: Effect of changing N_2 parameters, so that $\sigma_{11}=3.334$ Å and $\epsilon_{11}/k_B=96.01$ K, with σ_{22} and ϵ_{22}/k_B at their reference values.

effective relaxation frequencies (inverse relaxation times) are the eigenvalues of the matrix **A** in the relaxation equation, Eq. (12), the eigenvectors of which specify the normalized contribution of each species (see Ref. 17 for details and examples). The strong shift of the absorption peak due to the overall change in σ_{11} is not surprising given the large nitrogen concentration and the wide variation in $P^{10}(1,1)$ with σ_{11} [Fig. 3(a)]. On the other hand, the larger change in $P^{10}(2,2)$ with σ_{22} [Fig. 5(a)] as well as the stronger dependence of $P_{01}^{10}(1,2)$ on σ_{12} [Fig. 5(b)] are not enough to cause an absorption peak shift comparable to that due to the variation of the nitrogen collision diameter. We conjecture that this is the case due, first, to the very small water vapor concentration (338 ppm), and, second, to a possible ''buffering'' effect of methane with its 1534 cm^{-1} vibrational level which is quasiresonant with the 1596 cm^{-1} mode of water. In addition, the V-V transition probabilities between the two modes of methane considered and water are several orders of magnitude higher than the V-V probabilities between methane and nitrogen, which may also affect the attenaution.

The effect of the Lennard–Jones force constants on the acoustic attenuation may be more easily understood in terms of the behavior of the relaxation frequencies. The explicit dependence of the two main relaxation frequencies (normalized absorption peaks in Fig. 6) on the values of the nitrogen LJ parameters is shown in Fig. 7 ($f_{\mathrm{relax},1}$ and $f_{\mathrm{relax},2}$ refer to the frequencies of the first and second attenuation peaks, respectively). The large effect of the nitrogen collision diameter σ_{11} is obvious. Varying σ_{11} results in large changes in both relaxation frequencies by factors of 2.7 and 2.4 for $f_{\mathrm{relax},1}$ and $f_{\mathrm{relax},2}$, respectively. The change in the potential depth ϵ_{11} brings about a considerably smaller variation in the relaxation frequencies (about 10% or less). When the water LJ parameters are varied (not shown), the change in the collision diameter of water molecules σ_{22} brings about relatively small changes in the two main relaxation frequencies (about 5%); similarly, the effects of changing ϵ_{22} amount to less than 1%. The dependence of the two relaxation peaks on σ_{11} is slightly nonlinear, apparently related to the sensitivity of the transition probabilities to the potential parameters (Fig. 3).

If the 1% molar fraction of methane is replaced by nitrogen so that the new mixture is 338 ppm water and the rest nitrogen, and the Lennard–Jones parameters of the two constituents are allowed to vary as before, the effect on the relaxation curves changes drastically: Water now dominates the sensitivity of the mixture. In this case, changes in both the water and nitrogen collision diameters σ_{22} and σ_{11} induce considerable shifts of the main relaxation frequency, as shown in Fig. 8. As in the case of the ternary mixture, the variations in the N_2-H_2O mixture attenuation due to changes in ϵ_{11} and ϵ_{22} are insignificant, and therefore are not shown. The behavior of the main relaxation frequency as a function of the LJ parameters of water and nitrogen (not shown) is similar to that shown in Fig. 7.

The difference in the degree of the impact of changing σ_{22} between the attenuation curves in Figs. 6 and 8 could be explained in terms of the vibrational factors, which are proportional to the ratio of vibration amplitudes and frequencies and play a significant role in the evaluation of transition probabilities.[26] Table I indicates that the vibrational factor of the nitrogen molecules is more than one order of magnitude smaller than those of the other species present in the mixture. The lightest of the three gases, methane, has the highest vibrational factor. The 1534 cm^{-1} mode of methane very likely couples near resonantly with the 1596 cm^{-1} mode of water. As a result, changing the force constants of water does not amount to a sizable effect on the relaxation curve in Fig. 6. However, when the methane is entirely replaced by nitrogen, water molecules lose a ''favorite'' interaction partner, with a commensurately high vibration factor. The water-nitrogen mixture is a composition of extremes: Very small amounts of water are able to ''push'' the relaxation frequency from that of pure nitrogen (<0.1 Hz/atm) (Ref. 27) to around 6–7

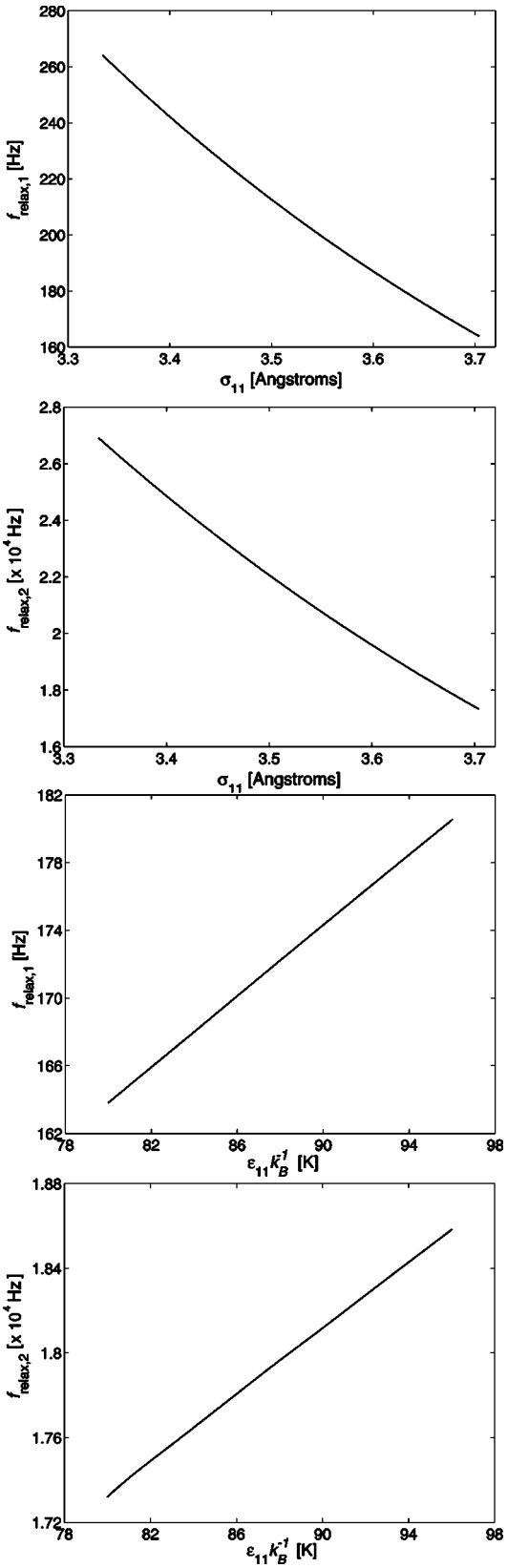

FIG. 7. Dependence of the two main relaxation frequencies (normalized absorption peaks in Fig. 6), at $P_0=1$ atm, on the values of the LJ parameters of nitrogen. Note the higher sensitivity of the relaxation frequencies to σ_{11}.

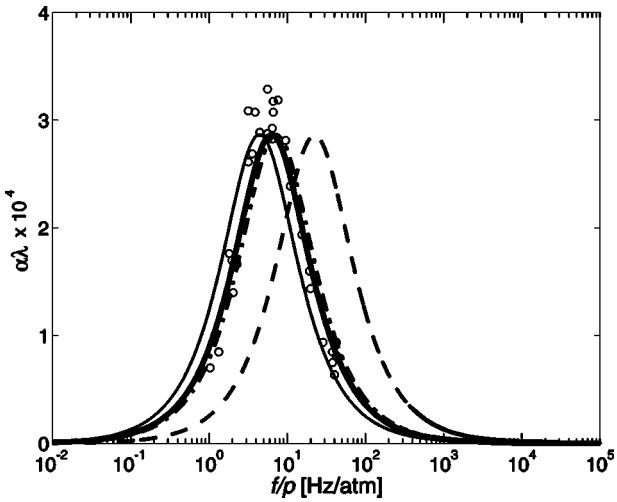

FIG. 8. Effects of the variation of the collision diameter for a mixture of 338 ppm H_2O and the rest N_2, on the normalized attenuation. Thin solid: using reference values for $\sigma_{11}=3.704$ Å and $\sigma_{22}=4.468$ Å (Table II). Dashed: effect of 28% change of σ_{22} from its reference value of 4.468 Å to 3.217 Å. Dot-dashed: effect of 10% change of σ_{11} from its reference value of 3.704 to 3.334 Å. Circles: experimental data of Zuckerwar and Griffin (Ref. 28). Bold solid: using $\sigma_{11}=3.704$ Å and $\sigma_{22}=4.200$ Å (6% change from reference value).

Hz/atm. Beside the large changes induced by the large quantity of heavy nitrogen molecules, varying the potential parameters of the water molecules, which are characterized by a considerably higher vibration factor, shifts the relaxation frequencies to a large extent.

Experimental data obtained by Zuckerwar and Griffin[28] for the same nitrogen-water vapor mixture is also plotted. By slightly adjusting the hard-sphere collision diameter σ of water or nitrogen, the absorption curve can be made to agree very well with the data. As an example, by making the water collision $\sigma_{22}=4.200$ Å (a 6% change from its reference value), the predicted curve can be made to agree fairly well with the data.

IV. CONCLUSIONS

The paper addresses acoustic propagation in gaseous media, associated with vibration-translation and vibration-vibration relaxation, as influenced by the choice of the Lennard–Jones parameters. Although certain molecular interaction specifics are described in some detail, the drive behind the current work is acoustics, specifically the ongoing quest for precise acoustic propagation models to be used in gas sensing applications.

The salient point of the SSH-Tanczos treatment of molecular relaxation in gases is the approximation of the Lennard–Jones interaction potential by a shifted exponential function in the vicinity of the classical turning point. The probability of quantum transitions between vibrational levels depends nontrivially on the Lennard–Jones potential depth ϵ and hard-sphere collision diameter σ. However, the values for both ϵ and σ can vary substantially in the literature, since they are quite difficult to measure. What has not been clear is how these variations in the fundamental collision parameters play out with regard to the values for the shifted exponential repulsion parameter α^* and the classical turning point r_c, which, in turn, affect the transition probabilities and subsequently the acoustic attenuation. Furthermore, in multicom-

ponent gas mixtures, these two parameters interact such that a small variation in one of the parameters of the intermolecular energy (here, approximated by the Lennard–Jones potential) could result in a large change in the acoustic attenuation in the mixture.

To address the sensitivity of the acoustic attenuation in gas mixtures to the Lennard–Jones parameters, the exchange of energy with translation is treated via a full pairwise parametrization of the transition probabilities, assuming binary collisions. The shifted-exponential parameters α^* and r_c depend on the choice of the Lennard–Jones parameters, ϵ and σ. The specific choice of these parameters affects the transition probabilities and, subsequently, the acoustic attenuation (and phase velocity) in model mixtures of nitrogen, methane, and water vapor. The behavior of the transition probabilities as a function of changing the values of the LJ parameters (decreasing with increasing collision diameter, and increasing with potential depth—see Figs. 3 and 5) can be explained, in a conjectural context, starting with the behavior of the repulsion parameter and classical turning point. Figures 2 and 4 show that r_c increases with both σ and ϵ, while α^* decreases with increasing σ and increases with ϵ. An increasing r_c means that the point where two ''colliding'' molecules transfer their relative kinetic energy to potential energy occurs at smaller separations. The parameter α^* is the ''slope'' of the shifted-exponential potential function. It determines the ''strength'' of the interaction potential: Large values of α^* imply ''strong'' interaction, while small values of α^* imply ''weak'' interaction. Thus, as the value of the collision diameter σ increases, it can be conjectured that there is a progressively weaker interaction occurring at progressively shorter intermolecular separations; hence the decrease in the transition probabilities. On the other hand, an increasing potential depth ϵ leads to a progressively stronger interaction at shorter separations and thus to an increase in the transition probabilities. The transition probabilities are extremely sensitive to the value of collision diameter σ rather than to the depth of the Lennard–Jones potential well ϵ. The sensitivity of the acoustic relaxation model to the choice of an LJ parameter (the collision diameter for water, for the mixture considered) is itself ''sensitive'' to the concentration of the molecular species making up the mixture.

ACKNOWLEDGMENTS

The authors gratefully acknowledge the support of NASA (Grant No. NAG9-1544) as well as fruitful discussions with Douglas Shields.

[1] S. Phillips *et al.*, ''Theory for a gas composition sensor based on acoustic properties,'' Meas. Sci. Technol. **14**, 70–75 (2003).
[2] S. G. Ejakov *et al.*, ''Acoustic attenuation in gas mixtures with nitrogen: experimental data and calculations,'' J. Acoust. Soc. Am. **113**, 1871–1879 (2003).
[3] F. London, ''The general theory of molecular forces,'' Trans. Faraday Soc. **33**, 8–26 (1937).
[4] R. P. Feynman, ''Forces in molecules,'' Phys. Rev. **56**, 340–343 (1939).
[5] J. O. Hirschfelder, C. F. Curtiss, and R. B. Bird, *Molecular Theory of Gases and Liquids*, Chap. 13, Wiley, New York, 1964.
[6] L. Landau and E. Teller, ''Zur Theorie der Schalldispersion,'' Phys. Z. Sowjetunion **10**, 34–43 (1936).
[7] J. M. Jackson and N. F. Mott, ''Energy exchange between inert gas atoms and a solid surface,'' Proc. R. Soc. London **137**, 703–717 (1932).
[8] F. D. Shields, ''Thermal relaxation in carbon dioxide as a function of temperature,'' J. Acoust. Soc. Am. **29**, 450–454 (1957).
[9] K. F. Herzfeld and T. H. Litovitz, *Absorption and Dispersion of Ultrasonic Waves*, Chap. 8, Academic Press, New York, 1959.
[10] R. N. Schwartz, Z. I. Slawsky, and K. F. Herzfeld, ''Calculation of vibrational relaxation times in gases,'' J. Chem. Phys. **20**, 1591–1599 (1952).
[11] R. N. Schwartz and K. F. Herzfeld, ''Vibrational relaxation times in gases (three-dimensional treatment),'' J. Chem. Phys. **22**, 767–773 (1954).
[12] F. I. Tanczos, ''Calculation of vibrational relaxation times of the chloromethanes,'' J. Chem. Phys. **25**, 439–447 (1956).
[13] F. J. Krieger, ''The viscosity of polar gases,'' Project Rand Report RM-646, July, 1, 1951.
[14] L. Monchick and E. A. Mason, ''Transport properties of polar gases,'' J. Chem. Phys. **35**, 1676–1697 (1961).
[15] F. D. Shields, ''On obtaining transition rates from sound absorption and dispersion curves,'' J. Acoust. Soc. Am. **47**, 1262–1268 (1970).
[16] H.-J. Bauer, F. Douglas Shields, and H. E. Bass, ''Multimode vibrational relaxation in polyatomic molecules,'' J. Chem. Phys. **57**, 4624–4628 (1972).
[17] Y. Dain and R. M. Lueptow, ''Acoustic attenuation in three-component gas mixtures—theory,'' J. Acoust. Soc. Am. **109**, 1955–1964 (2001).
[18] Y. Dain and R. M. Lueptow, ''Acoustic attenuation in a three- gas mixture—results,'' J. Acoust. Soc. Am. **110**, 2974–2979 (2001).
[19] C. B. Moore, ''Vibration-rotation energy transfer,'' J. Chem. Phys. **43**, 2979–2986 (1965).
[20] H. E. Bass, J. R. Olson, and R. C. Amme, ''Vibrational relaxation in H_2O vapor in the temperature range 373–946 K,'' J. Acoust. Soc. Am. **56**, 1455–1460 (1974).
[21] H. K. Shin, ''Vibration-to-rotation energy transfer in water, heavy water, and ammonia,'' J. Phys. Chem. **77**, 346–351 (1973).
[22] H. K. Shin, ''Self-relaxation of vibrationally excited H_2O molecules,'' J. Chem. Phys. **98**, 1964–1978 (1993).
[23] A comprehensive database of past and current studies of water structure is available at www.lsbu.ac.uk/water
[24] J. M. Prausnitz, *Molecular Thermodynamics of Fluid-Phase Equilibria*, Prentice-Hall, New Jersey, 1969, p. 72.
[25] J. D. Lambert, *Vibrational and Rotational Relaxation in Gases*, Clarendon Press, Oxford, 1977.
[26] Ref. 25, p. 46.
[27] A. J. Zuckerwar and W. A. Griffin, ''Resonant tube for measurement of sound absorption in gases at low frequency/pressure ratios,'' J. Acoust. Soc. Am. **68**, 218–226 (1980).
[28] A. J. Zuckerwar and W. A. Griffin, ''Effect of water vapor on sound absorption in nitrogen at low frequency/pressure ratios,'' J. Acoust. Soc. Am. **69**, 150–154 (1981).